A Selective Negative Derivative Feedback algorithm to improve stability for inertial actuators

N. Debattisti[a], M. L. Bacci[a], S. Cinquemani[a]

[a] Politecnico di Milano, Dipartimento di Meccanica, Via La Masa 1, 20156 Milano, Italy.

ABSTRACT

Inertial actuators are widely used in active vibration control, since they don't need to react off the base structure. Then, unlike reactive actuators, they can be used as modules that can be directly installed on a vibrating structure. In many cases, inertial actuators are used to develop some stand-alone active dampers. Such devices are embedded with sensors and a microcontroller, in order to independently perform the vibration control task. This kind of control unit is commonly adopted to implement decentralized architectures. In this work, the main goal was to limit instability phenomena related to the dynamics of inertial actuators. The proposed solution also aims to improve the performance of a decentralized control strategy through a partial sharing of data between devices, without the use of cables. First, the formulation of the modified Negative Derivative Feedback resonant controller is derived; then, the steps of the control strategy are explained, which are based on a preliminary modal identification of the structure and the assignment of a compensator for each resonance frequency to be controlled. Finally, the proposed method is validated with experimental results from a clamped-clamped beam.

Keywords: Vibration control, Inertial actuators, Control algorithms, Wireless sensors, Automation

1. INTRODUCTION

Among the different solutions adopted in structural vibrations control, active control systems can be a valid alternative to passive dampers, as they provide higher performance, especially for low-frequency applications. To date, the most used active control strategies are based on centralized architectures in which, as the size of the control system increases, logistical and implementation problems can occur, representing a limitation.[1] In a totally decentralized control logic, on the contrary, devices act as self-sufficient local controllers: since there is no share of information, the control action will depend only on local information, resulting in lower performance with respect to the centralized case.

These architectures require a complex setup of all the components involved in the control task: many sensors and actuators have to be installed and wired to a real-time board, which manages the input signals coming from sensors and, through the implementation of the control logic, the output signals to provide to the actuators. To overcome this problem, a stand-alone device has been developed, which is fitted with all the necessary elements to work in an autonomous way: there are *sensors* for the data acquisition, an *microcontroller* in which the control algorithm is implemented and the *actuator*, driven by the board.

In this study, proof-mass actuators are used and their dynamics result in some limitations on the performance of the controlled system. An inertial actuator behaves like an ideal force generator only when the excitation frequency is higher than its natural frequency. In the other case, the force transmitted to the structure has a low module and it is in counter-phase with respect to the control force, leading to instability problems.[2–4] Therefore, the design phase of the control law has been carried out in order to achieve two main goals:

- to limit instability phenomena related to the dynamics of inertial actuators;
- to improve the overall quality of the vibration control of a totally decentralized architecture through the share of information between the control units;

Further author information: (Send correspondence to Simone Cinquemani)
E-mail: simone.cinquemani@polimi.it Telephone: +39 (0)2 2399.8454

To allow an easy placement of smart dampers and to avoid complex setup, wireless communication is used instead of wired connections. However, the use of this technology involves some non-negligible complications, like data loss and transmission delay.[5–7] These phenomena commonly occur when the communication channel is saturated and they may affect the stability of the controlled system.[8,9] The proposed control strategy, based on the *Skyhook* damping[10,11] and resonant control[12,13] techniques, is able to automatically adapt to the type of structure and the nature of the vibration to control, resulting in a coordinated control action between devices within the network.

The paper is structured as follows. In Section 2 the features of the stand-alone device are presented, while in Section 3 the formulation of the control algorithm is derived and its functioning principle is explained. In Section 4 the experimental results obtained on a large vibrating system are shown. Finally, conclusions are drawn in Section 5.

2. THE STAND-ALONE DEVICE

The developed device is able to carry out operations of vibration control in an autonomous way. In Fig. 1 is shown the prototype which has been realized. Two Micro Electro-Mechanical Systems (MEMS) digital accelerometer are available: one is placed on the fixed frame of the device (soldered on the board) and the other on the suspended mass of the actuator. The first sensor measures the acceleration of the structure, which will be used to compute the control signal, while the second one measures the acceleration of the actuator, in order to get information about its dynamics during the control action. This feature is useful to detect a stroke saturation condition.[14–16]

These signals are acquired by the microcontroller, the main element of the Printed Circuit Board (PCB) in which different control algorithms can be implemented.[17,18] Since the data-ready interrupt of the sensor placed on the board is triggered at 1600 Hz, the real-time control loop runs at that frequency. The output of the control algorithm is the command signal which drives the actuator. This signal must be converted from the digital to the analog domain, conditioned and amplified by the analog and power stages (see the *Analog and Power Conditioning* block in Fig. 2). The actuation system consists in a magnetodynamics inertial actuator,[19–21] which has been modeled as a mass-spring-damper 1-Degree Of Freedom (DOF) system. The electromagnetic force applied on the suspended mass is the result of the interaction between a variable magnetic field and a permanent magnetic field. Inertial actuators do not need to react off the base structure, so they can be used as modules that can be directly installed on a vibrating structure. One of the several cases in which a similar device could be

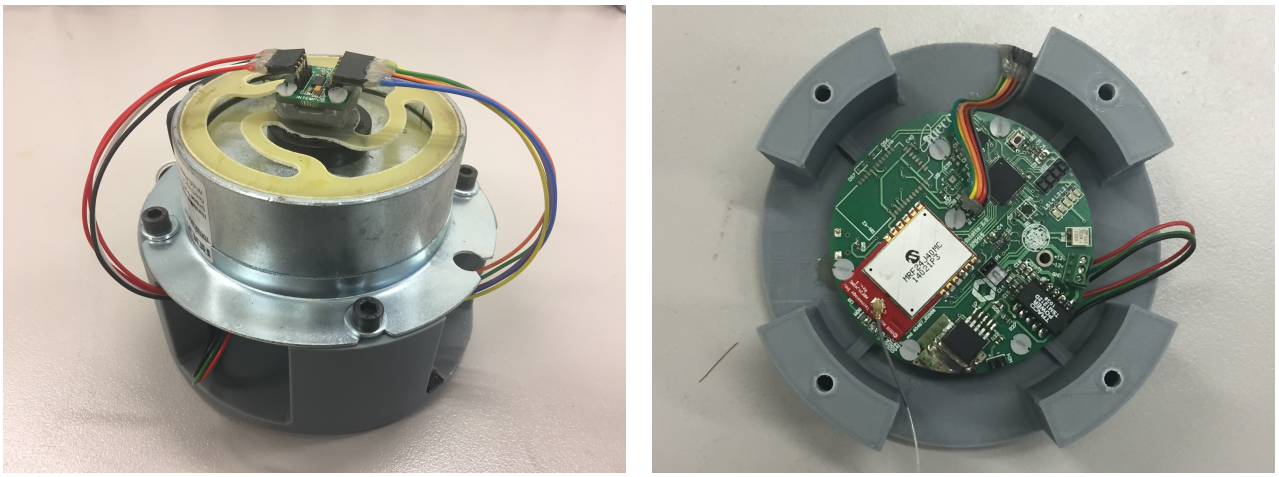

(a) (b)

Figure 1: First prototype of the stand-alone device (a) and particular of the board (b)

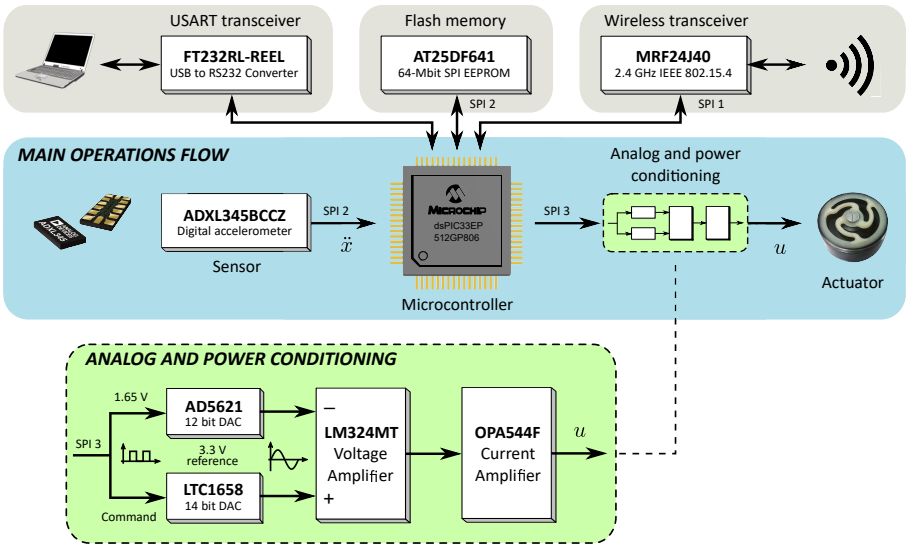

Figure 2: Block diagram which represents how the board is designed

employed regards the problem highlighted in,[22] which is related to the undesired noise and vibrations generated by engines and exhaust stacks of cruise ships.

The PCB is also provided with a wireless module, which allows the device to communicate with the others within the network (both transmission and reception). The wired communication (USB) with the computer is needed for the firmware loading and for the transmission of commands in order to manage the operations of the board. Moreover, it is possible to read and acquire data from sensors.

3. CONTROL ALGORITHM FORMULATION

The control law which is proposed in this work has been developed according to the two requirements highlighted in Section 1. The first step consists on the derivation of a resonant control which calculates the feedback forces through a dynamic compensator. This strategy allows to successfully limit the negative effect of the dynamics of the inertial actuator which affects the stability of the controlled system.

3.1 Derivation of the resonant controller

The general equation of motion of a controlled n-DOF system can be written in modal coordinates through the modal matrix $\Phi \in \mathbb{R}^{n \times n}$. As in most cases, the whole system dynamics is not taken into account. Then, a reduced model of the system has been defined considering a small set of decoupled modal coordinates ($n_R < n$). The i^{th} modal equation, which represents the contribution of the i^{th} mode on the system dynamics, is defined as:

$$\ddot{q}_i + 2\zeta_i \omega_i \dot{q}_i + \omega_i^2 q_i = u_{c,i} + d_i \qquad \text{with} \qquad i = 1, \dots, n_R \tag{1}$$

where q_i is the i^{th} modal coordinate, ζ_i and ω_i are the damping ratio and natural frequency associated to the i^{th} mode, while $u_{c,i}$ and d_i are the generalized control and disturbance forces acting on the i^{th} mode.

The Negative Derivative Feedback (NDF) compensator is designed to be robust to spill-over effects related to higher and lower modes with respect to the controlled ones and it is based on the negative feedback of the modal velocity.[12] Calling η_i the DOF of the i^{th} mode compensator, the control force for the i^{th} controlled mode can be written as:

$$\begin{cases} u_i = -g_i \dot{\eta} \\ \ddot{\eta}_i + 2\zeta_i \omega_i \dot{\eta}_i + \omega_i^2 \eta_i = k_i \left(\dot{q}_i - \dot{\eta}_i \right) \end{cases} \tag{2}$$

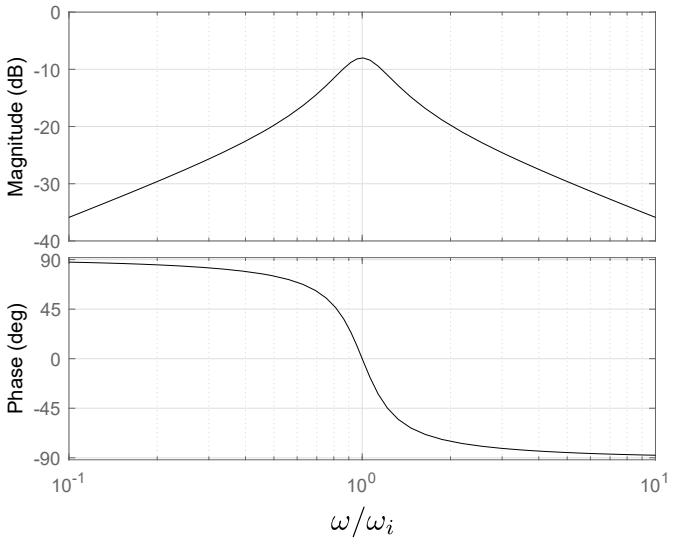

Figure 3: Frequency Response Function (FRF) of the Negative Derivative Feedback compensator normalized on the compensator resonance frequency ω_i

where ζ_i and ω_i are the damping ratio and eigenfrequency of the compensator respectively (which are equal to the ones of the i^{th} controlled mode), while g_i and k_i are two gains. So, the transfer function between modal velocity and control force becomes:

$$\frac{U_{c,i}(s)}{\dot{Q}_i(s)} = -\frac{k_i g_i s}{s^2 + (2\zeta_i\omega_i + k_i)\, s + \omega_i^2} \tag{3}$$

and it represents the transfer function of a band-pass filter centered on the mode resonance frequency (Fig. 3).

In conclusion, the band-pass formulation of this kind of compensator allows the NDF to be robust, by filtering out higher and lower frequency disturbances (especially lower frequencies). For this reason, the control gains can be increased with respect to other types of resonant controllers, achieving better performance in terms of vibrations reduction and damping increase.

3.1.1 Continuous-to-discrete domain conversion equations

The continuous-time transfer function of the compensator is dependent from the resonance frequency ω_i and the damping ratio ζ_i of the i^{th} mode. The implementation of this function on the electronic board requires the conversion from the continuous to the discrete domain. The goal is to make the process adaptive, which means setting the compensator in every situation in an autonomous way. Thus, the equations that relate the resonance frequency and the damping ratio to the correct values of the coefficients of the discrete transfer function have been obtained. Moreover, a modified version of the compensator previously defined is presented.

Eq. 3 represents the compensator transfer function. The shape of this compensator, as previously said, depends on the damping ratio ζ_i, on the frequency ω_i at which it is centered and on the two gains k_i and g_i. In order to move from continuous time to discrete time definition of the compensator, the transfer function in Z-domain assumes this form:

$$\tilde{C}_i(z) = \frac{az + b}{z^2 + cz + d} \tag{4}$$

A mathematical model for the computation of the coefficients into the Eq. 4 has been derived. The coefficients will be defined according to the frequency of the vibration modes identified in the frequency range of interest. The equations of this model are reported in Table 1, in which the parameter T represents the sampling interval. The

module of the compensator transfer function is maximum near the resonance frequency ω_i and the magnitude depends on the resonance frequency itself. For this reason, the acceleration signal will be amplified or damped, according to the frequency on which the compensator is set. In order to solve this problem, the definition of the compensator has been slightly changed. The modified transfer function is defined in this way:

$$\tilde{C}_i^*(s) = \frac{(2\zeta_i\omega_i + k_i)\, s}{s^2 + (2\zeta_i\omega_i + k_i)\, s + \omega_i^2} \tag{5}$$

where the numerator and denominator orders are not changed and thus the parameters have the same meaning of the previous case.

The useful feature of this modified compensator is that its maximum module (which is still in correspondence of ω_i) is around 0 dB in any case, regardless of the value of the resonance frequency. Also in this case, the parameters of the Z-Transform can be determined by means of the model in Table 1, except for the first one, which is now defined as follows:

$$a = \frac{2\zeta_i + \frac{k_i}{\omega_i}}{\sqrt{1 - \left(\zeta_i + \frac{k_i}{2\omega_i}\right)^2}} \cdot e^{-\left(\zeta_i\omega_i + \frac{k_i}{2}\right)T} \cdot \sin\left(\sqrt{1 - \left(\zeta_i + \frac{k_i}{2\omega_i}\right)^2}\,\omega_i T\right) \tag{6}$$

What has been said before about the difference between the two compensators can be better appreciated looking at Fig. 4. The behaviour of the compensators transfer functions by varying the resonance frequency ω_i is reported for both configurations. This demonstration is merely qualitative (the chosen frequencies have no physical meaning for this study), in order to clearly show how the transfer functions vary with frequency. In Fig. 4a is represented the trend of the first compensator presented (Eq. 3), while in Fig. 4b is represented the trend of the modified version of the band-pass filter (Eq. 5).

3.2 Control strategy

The idea on which the proposed control strategy is based focuses on improving the performance of a totally decentralized control architecture by means of a strategic utilization of the wireless channel available on each device. The feature introduced in Section 3.1.1 to automatically adapt the compensator according to the desired parameters can be merged with the information coming from a preliminary modal analysis. Such analysis is performed by the actuators placed on the structure and, in this way, it is possible to develop a specific control action without any prior knowledge of either the system or the disturbing forces acting on the system itself.

3.2.1 Preliminary modal identification

The first step consists of a preliminary identification of the vibration modes of the system. This analysis is performed by using the actuators as a disturbance source, in order to excite the structure in a given range of frequencies. The shape of the Frequency Response Function and the eigenfrequencies which are detected depend

$$\begin{aligned}
a &= \frac{k_i g_i}{\omega_i\sqrt{1 - \left(\zeta_i + \frac{k_i}{2\omega_i}\right)^2}} \cdot e^{-\left(\zeta_i\omega_i + \frac{k_i}{2}\right)T} \cdot \sin\left(\sqrt{1 - \left(\zeta_i + \frac{k_i}{2\omega_i}\right)^2}\,\omega_i T\right) \\
b &= -a \\
c &= -2e^{-\left(\zeta_i\omega_i + \frac{k_i}{2}\right)T} \cdot \cos\left(\sqrt{1 - \left(\zeta_i + \frac{k_i}{2\omega_i}\right)^2}\,\omega_i T\right) \\
d &= e^{-(2\zeta_i\omega_i + k_i)T}
\end{aligned}$$

Table 1: Equations for the conversion from s-Transform to Z-Transform

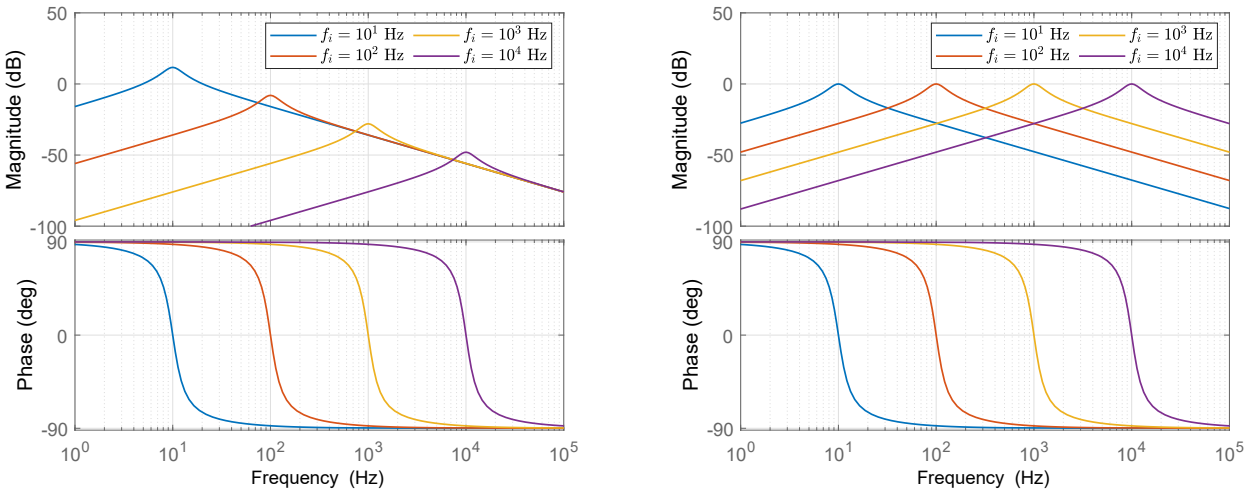

Figure 4: Transfer function trend in frequency of the compensators defined in (a) Eq. 3 and (b) Eq. 5

on the position of the actuators along the structure. For a given vibration mode and a given actuator, the position of the latter determines if it can absorb the energy when that mode is excited. If the actuator is placed in a vibration node (for that specific mode), no oscillation can be measured at that specific frequency and no force can be generated to increase the damping of the structure.

To allow the actuators to generate a force with a frequency which varies with time, a "Sweep working mode" has been created. The disturbance action consists of a sine wave with constant module (which is set offline) and variable frequency. The starting frequency is set equal to 10 Hz, because below this value the acceleration is very low and the signal coming from the sensor is dominated by the noise. Then, the frequency is increased by 1 Hz each second, up to the maximum desired value (~ 250 Hz). While the structure is excited, it is necessary to sample the signal in order to perform the Fast Fourier Transform (FFT), thus obtaining the needed information in the frequency domain.

To carry out this preliminary identification, a series of operations must be performed one by one according to a specific order. To do this, the two devices must work in a synchronized way, communicating with each other through the wireless channel. In order to simplify the operations management, one device is chosen as a *master*, which makes decisions based both on its own information and the ones it has received. The second device is set to be a *slave*, which communicates its information to the master and executes the instructions received from the master itself.

So, the first of these operations is the sweep excitation of the structure and the simultaneous calculation of the FFT of the acceleration signal performed by the master. When the sweep excitation is over, the result obtained is a set of points which outlines the trend of the FRF of the system in the considered frequency range, in terms of frequency and module. An algorithm for the peaks recognition has been developed, in order to analyze the shape of the FRF and to extract useful information such as resonance frequencies and related modules. Once the "local" vibration modes have been collected, which are the subset of the vibration modes of the structure perceived by the device placed in that particular position, the master sends to the slave the command to start the sweep excitation. As previously done by the master, also the slave performs the identification obtaining its own "local" vibration modes and then it sends the result to the master.

In the next step, the master compares its information on the modes with the ones received from the slave. Another algorithm has been developed, which compares one by one the resonance frequencies obtained by the two devices and, when it finds a frequency that in the other device is missing, adds it to the list and continues the

comparison. Once this phase is completed, the master sends the updated vector containing the vibration modes to the slave, and both devices set a compensator like the one described in Section 3.1.1 for each resonance frequency. From now on, the microcontroller will apply to the measured acceleration n_R independent compensators, thus obtaining n_R different signals (with n_R equal to the number of identified vibration modes). By integrating each of these signals, it will obtain n_R velocity values, each having a different frequency (corresponding to the resonance frequencies). These operations are summarized in Fig. 5a and they are performed at the beginning, when the structure is not excited by the disturbance forces.

3.2.2 Devices control tasks planning

The second part of this chain of operations, instead, is carried out when the system is subjected to the external forces (Fig. 5b, from the time instant t^* on). In this phase, the master performs the FFT of the structure acceleration and, at the same time, it sends to the slave the command to start the same operation. The two devices analyze concurrently the actual vibration state of the system in their respective positions and they derive the information in the frequency domain by means of the FFT. Then, both devices analyze the result by recognizing the excited eigenfrequencies. At the end, the slave sends its results (in terms of frequency and module) to the master, which will compare them with its own.

Considering the information available at this point, the master will decide how to manage the global control law in order to make it as efficient as possible. In Fig. 6 is represented the diagram which better clarifies how the computation of the control signal that will be sent to the actuator takes place. Assuming that n_m vibration modes have been identified, as explained before the original signal of the measured acceleration $\ddot{x}_j$ of the j^{th} device is filtered by n_m different compensators. Then, the filtered signals $\ddot{\tilde{x}}_{j,i}$ are integrated and multiplied by

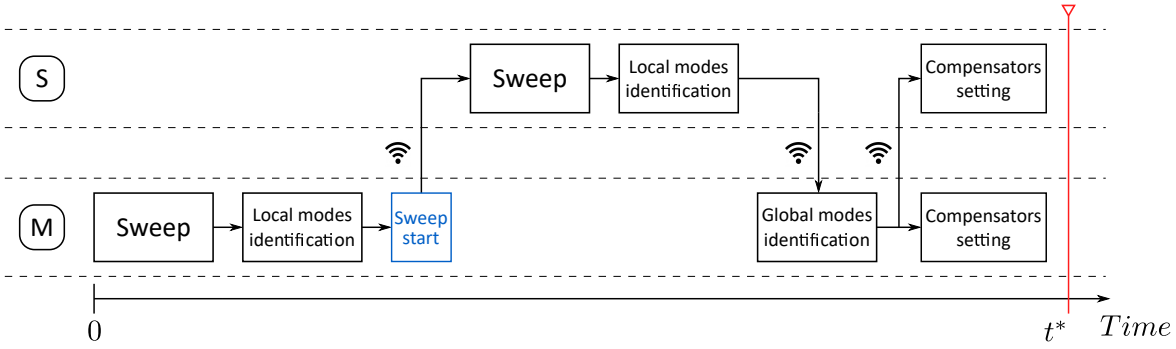

(a)

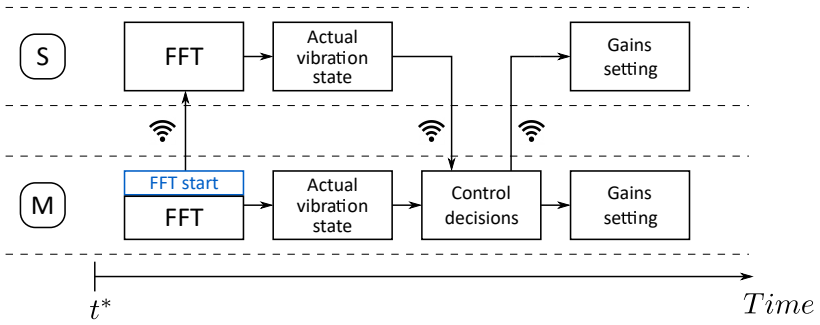

(b)

Figure 5: Block diagrams representing the operations performed by the master (M) and the slave (S) without (a) and with (b) the disturbance action

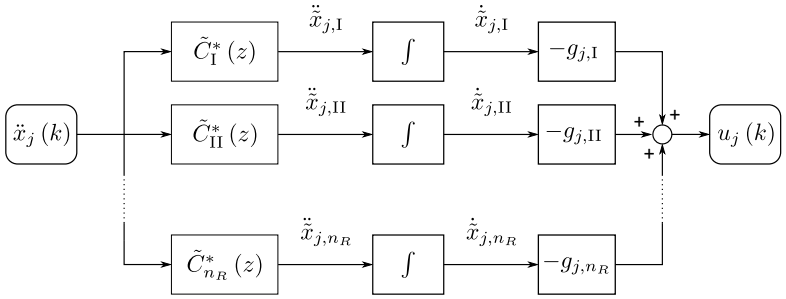

Figure 6: Block diagram representing how the control signal is obtained

the control gains $g_{j,i}$. The command signal u_j at the given time instant k can be written as follows:

$$u_j\,(k) = -\sum_{i=\mathrm{I}}^{n_m} g_{j,i}\dot{\tilde{x}}_{j,i}\,(k) \tag{7}$$

At this point, all the control gains $g_{j,i}$ with $i = \mathrm{I}, \ldots, n_m$ are temporarily set equal to zero. Now, the master decides which are the gains to be set different from zero in both devices and which are the values to be assigned to them. This kind of approach has been developed in order to self-adapt the control action according to the excited vibration modes and the position of the actuators with respect to the modes shape.

In a totally decentralized control architecture only local information are available. The proportionality between the control force and the local velocity is kept constant over the whole frequency range, since the feedback gain is always the same. Now, consider the following situation: the structure is subjected to external forces and two vibration modes are excited at the same time. Furthermore, suppose that one of the two devices is placed in a nodal position of one of the two modes. The other one, instead, is able to perceive both resonance frequencies. In this case, a device will act only on one mode, while the other will generate a force that will depend on both frequencies involved. The result will be that the vibration at one of the two frequencies will be very damped, while the other one will be subjected to a lower reduction. This happens because the vibration at one frequency is controlled by two devices while the other one is controlled only by one of them. Moreover, the feedback loop gain is lower if the actuator deals with two modes instead of one. The second condition occurs because an inertial actuator can absorb a limited amount of energy. By keeping the same gain, if two resonance frequencies are excited instead of one, the amount of energy that the actuator is asked to dissipate is higher. Therefore, in that case, it is necessary to decrease the gain of the control loop, in order to avoid instability problems or excessive control forces which could cause a stroke saturation. The one just described is the case which has been studied to assess the performance of the proposed control strategy.

Parameter	**Symbol**	**Value**	**Units**
Beam length	L	2.37	m
Beam height	h	0.02	m
Beam width	w	0.08	m
Cross-section	A	0.016	m^2
Young modulus	E	190	GPa
Density	ρ	7900	$\frac{\mathrm{kg}}{\mathrm{m}^3}$
Inertia moment	J	5.452×10^{-8}	m^4
Mass	m	12.73	$\frac{\mathrm{kg}}{\mathrm{m}}$

Table 2: Structural parameters of the beam

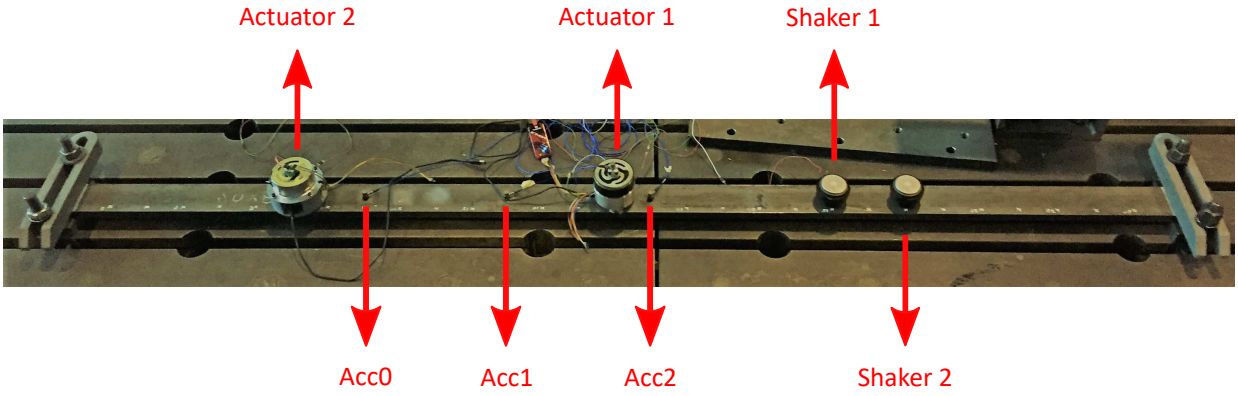

Figure 7: Experimental test rig

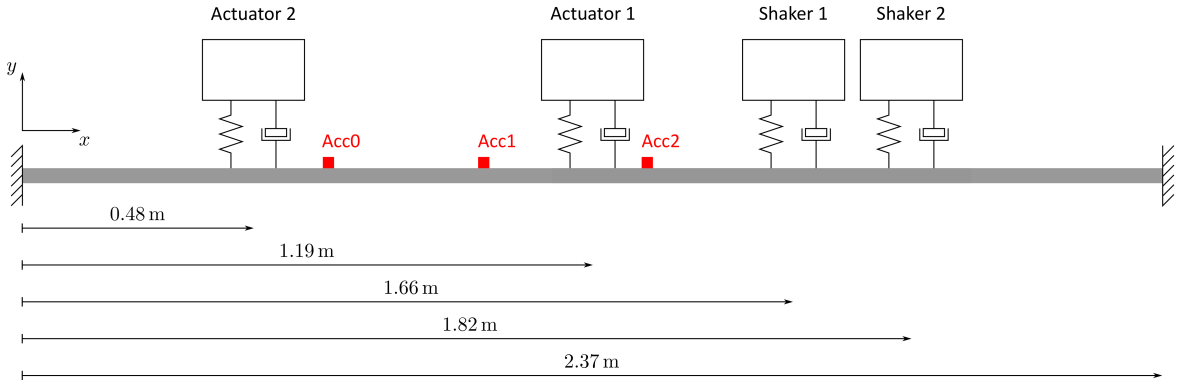

Figure 8: Configuration scheme of the beam

4. EXPERIMENTAL RESULTS

In order to verify the performance of this approach, some tests have been performed on a steel beam with a rectangular cross section, clamped on its ends; the parameters of the beam are summarized in Table 2. The length of this beam allows to place two stand-alone devices (*Actuator 1* and *Actuator 2*) and two shakers (*Shaker 1* and *Shaker 2*), as shown in Fig. 7 and Fig. 8. In Table 3 are reported some parameters of the inertial actuators used. Moreover, three analog accelerometers (*Acc0*, *Acc1* and *Acc2*) are mounted on the structure in order to the externally detect the vibration state in a global way. So, these sensors are not involved in the control loop. Their positions, according to the reference defined in Fig. 8, are 0.63 m, 0.95 m and 1.26 m respectively.

The results obtained with the solution proposed in Section 3.2 are shown below. The aim is to verify the possible improvements provided by a coordinated control in the case that more than one resonance frequency is

Parameter	**Sym**	**Device**			**Units**
		Shaker	**Actuator 1**	**Actuator 2**	
Resonance frequency	f_a	56.710	31.500	39.500	Hz
Damping ratio	ζ_a	0.049	0.049	0.030	-
Suspended mass	m_a	0.450	0.700	0.700	kg

Table 3: Inertial actuators parameters

Mode		I	II	III	IV	V
f_i [Hz]	**Num**	16.84	49.39	94.96	158.95	235.27
	Exp	17.02	49.08	94.72	159.11	235.51

Table 4: Resonance frequencies of the system obtained both numerically and experimentally

excited. The vibrations modes have been chosen in such a way one of the two devices could perceive only one of the two resonance frequencies, while the other could perceive both of them. This situation allows to set up:

- a totally decentralized architecture, in which each device generates a force proportional to all the harmonic components that it can measure
- a coordinated control architecture, in which one device will interact with a vibration mode while the second will interact with the other one.

In Section 3, all the phases of the devices setup process have been presented. The last of these phases concerns the setting of the control loop gains, which are managed by the master according to the vibration state of the structure detected by both devices. The vibration modes identified in the considered frequency range are reported in Table 4. In this case, the two vibration modes which have been chosen are III and V (94.72 Hz and

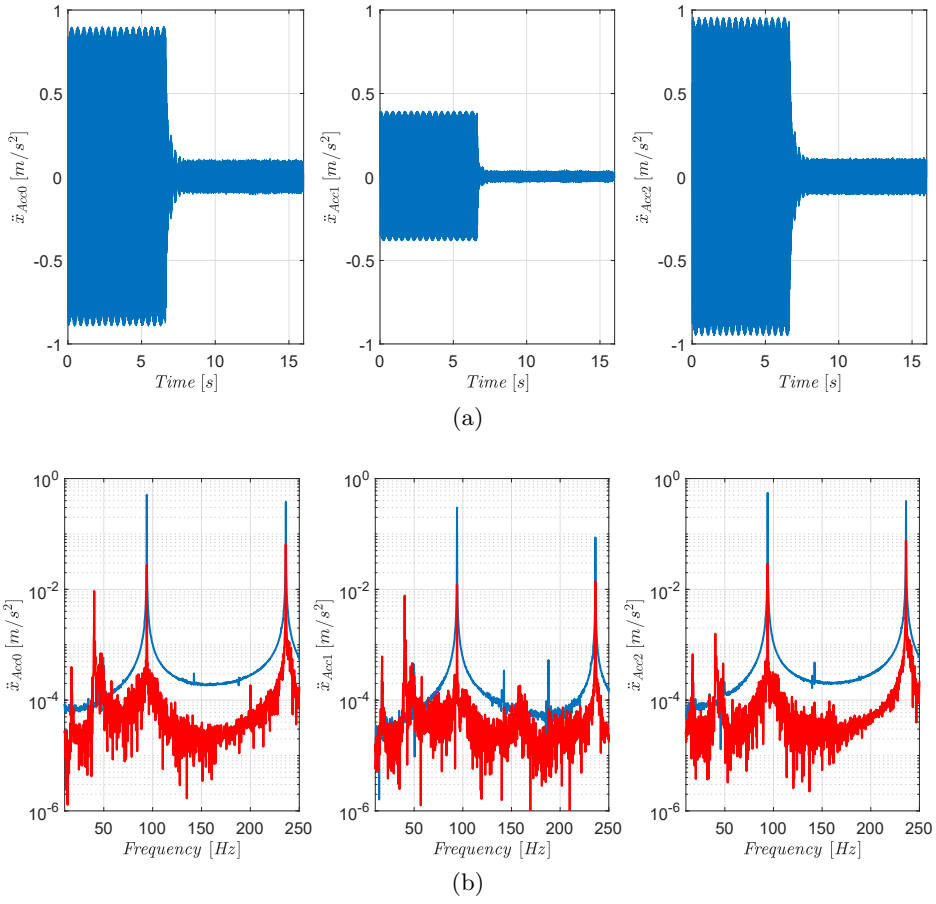

Figure 9: Experimental results obtained with the totally decentralized solution represented in (a) time domain and (b) frequency domain (uncontrolled and controlled case respectively in *blue* and *red*). First, second and third column represent accelerometers Acc0, Acc1 and Acc2 respectively

	Mode	Acc0	Acc1	Acc2
Uncontrolled	**III**	0.5088	0.2990	0.5526
	V	0.3805	0.0860	0.3931
Controlled	**III**	0.0276	0.0121	0.0290
	V	0.0638	0.0138	0.0754
Reduction %	**III**	94.5746	95.9515	94.7478
	V	83.2199	83.9406	80.8255

Table 5: Comparison of the FFT peaks values with the totally decentralized solution

235.51 Hz), due to their shape and the relative position of the two stand-alone devices. Actuator 1 can measure both the harmonics of the disturbance, while Actuator 2 can measure only the one of mode III. The disturbances have been set up by considering the position of the shakers with respect to the mode shapes. Then, Shaker 1 and Shaker 2 excite mode III and V respectively.

At the beginning, the classical decentralized control strategy has been implemented. Therefore, Actuator 1 will generate a force proportional to both harmonic components of the structure velocity via the same loop gain.

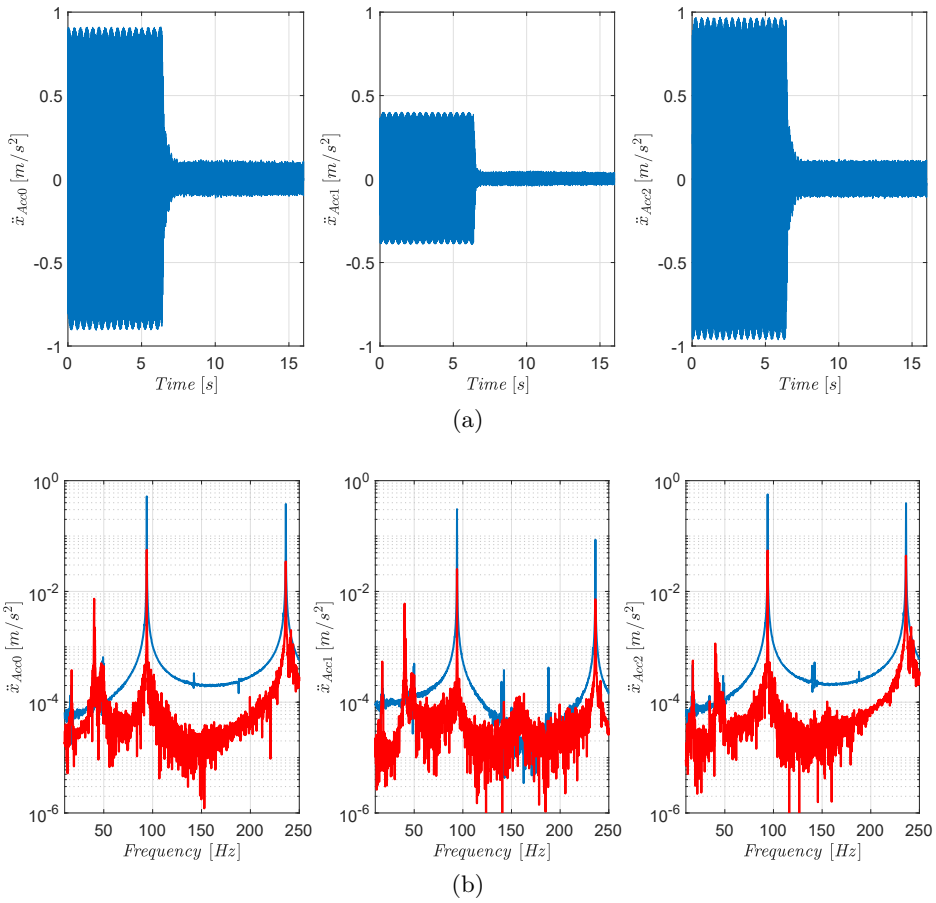

(a)

(b)

Figure 10: Experimental results obtained with the coordinated solution represented in (a) time domain and (b) frequency domain (uncontrolled and controlled case respectively in *blue* and *red*). First, second and third column represent accelerometers Acc0, Acc1 and Acc2 respectively

	Mode	Acc0	Acc1	Acc2
Uncontrolled	**III**	0.5203	0.3057	0.5652
	V	0.3791	0.0858	0.3918
Controlled	**III**	0.0564	0.0253	0.0548
	V	0.0347	0.0072	0.0441
Reduction %	**III**	89.1653	91.7222	90.3070
	V	90.8550	91.5960	88.7547

Table 6: Comparison of the FFT peaks values with the coordinated solution

In this phase of preliminary studies the aim was only to observe any difference between the two architectures. So, the feedback loop gain of both devices has been set at its maximum value, which has been obtained as a result of several tests. This value represents the threshold after which problems of instability or over-excitation may occur.

In Fig. 9 are shown the results obtained with this solution, in terms of acceleration time histories measured by the three sensors *Acc0*, *Acc1* and *Acc2* (9a) and the corresponding Fourier Transforms (9b). By observing the results coming from three different sensors allows to have a wider view of the vibration state of the structure, both in the uncontrolled and controlled case. In Table 5 the modules of the two harmonic components of the acceleration are collected. Data are reported for the three sensors, still distinguishing the uncontrolled case from the controlled one. Moreover, it is also shown the percentage reduction of the oscillation for the two excited frequencies. As can be seen by looking at percentage reductions, mode V is less damped than mode III, because at that frequency only one of the two actuators generates a force able to reduce the amplitude of the vibration. By considering mode III, instead, both actuators take part in the control action.

The coordinated control solution which has been proposed aims to improve the overall performance of the system by managing in a different way the computation of the control force in each device. Considering this particular case, an alternative way to manage the vibration control in a more global sense could be that in which each actuator acts to dampen only one of the two vibration modes. Since Actuator 2 can only detect the frequency of mode III, Actuator 1 will be arranged to work only at the frequency of mode V. In this way, the vibration related to those natural frequencies should be damped in a more uniform manner than in the previous case. In Fig. 10 are shown the results obtained with this kind of strategy, as well as in the totally decentralized case. The acceleration time histories and the corresponding Fourier Transforms are shown in Fig. 10a and Fig. 10b respectively, both for the uncontrolled and controlled system.

In Table 6 are collected the modules of the vibration harmonic components at the two resonance frequencies taken into account. Looking at the last two rows, it can be seen that the percentage reduction of the oscillation at both frequencies lies more or less on the same level (about 90%). These results confirm what has been said before, since the vibration of the structure is reduced in the same way for both the excited natural frequencies. Furthermore, an improvement can be noted also in quantitative terms by looking at the values in Table 7. At the expense of a worsening of the performance with respect to Mode III of about 5%, an improvement is obtained on the mode V of almost 8%. This is not only due to the different way in which the devices approach the control action, but it is also related to the fact that a higher feedback loop gain can be set to Actuator 1. The reason

	Mode	Acc0	Acc1	Acc2
Difference %	**III**	-5.4093	-4.2293	-4.4408
	V	+7.6351	+7.6554	+7.9291

Table 7: Comparison between the vibration reduction obtained with coordinated control with respect to the decentralized solution

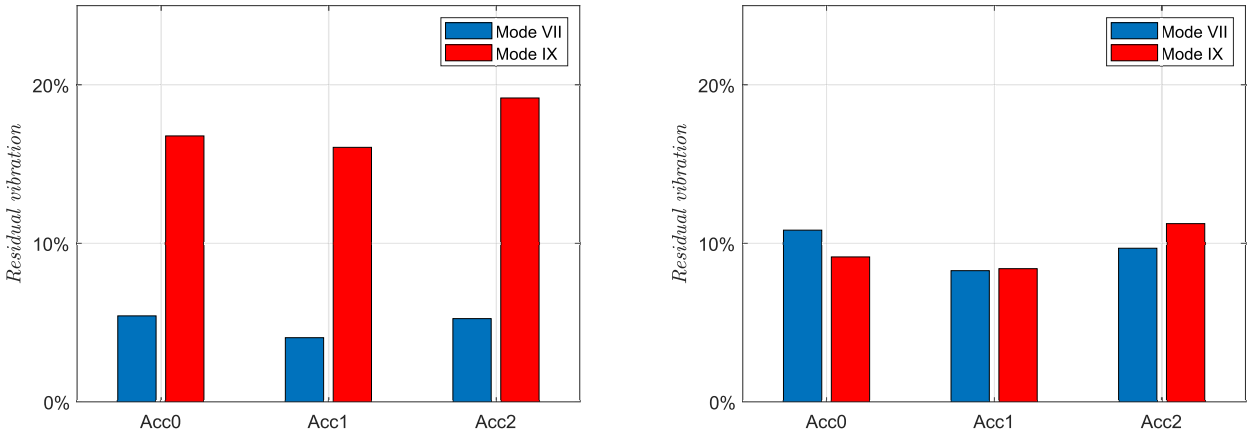

Figure 11: Comparison between the residual vibration of the modes III (*blue*) and V (*red*) in the totally decentralized (a) and coordinated strategy (b)

for this gain increase can be explained by referring to the concept of power absorbed by the actuator.[23]

Fig. 11 shows the histograms representing the percentages of residual vibration in the case of totally decentralized control (11a) and coordinated control (11b), in order to better appreciate the difference between the two. The percentages for mode III and mode V are shown in *blue* and *red* respectively.

5. CONCLUSIONS

This work has been mainly focused on the development of a solution that can exploit, in the most efficient way, the exchange of data between devices within their network. Particular attention has been also paid to the search for a solution to solve instability problems related to this kind of actuators, which represents the first step towards the realization of the final solution. The modified version of the digital band-pass filter which has been proposed allows to filter out the continuous contribution of the signal coming from the sensor. In the same way, components at higher frequencies become negligible. The implementation of the compensator also aims to limit the effect of the actuator dynamics on the control signal, which has been significantly reduced. The

The "*Selective Negative Derivative Feedback*" control algorithm allows the device to self-adapt its operating condition according to the characteristics of the structure on which it is mounted and the vibration to which the structure is subjected. When many devices are used, the sharing of specific types of data allows each device to extend its general overview of the system. One of the goals of this work was to ensure this sharing of information through a wireless network. In order to manage this situation, a *Master-Slave* architecture has been established. The device chosen as *Master* collects all the data coming from other devices and, once it analyzed them, sets a proper control strategy and communicates it to the *Slaves*. This strategy will be based on the control of specific vibration modes, which could be different between one device and another one. Such a situation allows the controlled system to be robust to stroke saturation phenomena, since components out of the selected range will be filtered out. The results obtained confirm that, in some situations, an improvement in the overall control action can be achieved compared to the totally decentralized case, thanks to a better management of resources.

REFERENCES

[1] Balas, M. J., "Feedback control of flexible systems," *IEEE Transactions on Automatic Control* **23**, 673–679 (1978).

[2] Paulitsch, C., Gardonio, P., and Elliott, S. J., "Active vibration damping using an inertial, electrodynamic actuator," *Journal of Vibration and Acoustics* **129**, 39–47 (2007).

[3] Elliott, S. J., Serrand, M., and Gardonio, P., "Feedback stability limits for active isolation systems with reactive and inertial actuators," *Journal of Vibration and Acoustics* **123**, 250–261 (2001).

[4] Benassi, L. and Elliott, S. J., "Global control of a vibrating plate using a feedback-controlled inertial actuator," *Journal of Sound and Vibration* **283**, 69–90 (2005).

[5] Ploplys, N. J., Kawka, P. A., and Alleyne, A. G., "Closed-loop control over wireless networks," *IEEE Control Systems Magazine* **24**(3), 58–71 (2004).

[6] Wang, Y., Lynch, J. P., and Law, K. H., "Decentralized h∞ controller design for large-scale civil structures," *Earthquake Engineering and Structural Dynamics* **38**, 377–401 (2009).

[7] Colandairaj, J., Irwin, G. W., and Scanlon, W. G., "Wireless networked control systems with qos-based sampling," *IET Control Theory & Applications* **1**(1), 430–438 (2007).

[8] Swartz, R. A. and Lynch, J. P., "Strategic network utilization in a wireless structural control system for seismically excited structures," *Journal of Structural Engineering* **135**, 597–608 (2009).

[9] Chu, S. Y., Soong, T. T., Lin, C. C., and Chen, Y. Z., "Time-delay effect and compensation on direct output feedback controlled mass damper systems," *Earthquake Engineering & Structural Dynamics* **31**(1), 121–137 (2002).

[10] Fuller, C., Elliott, S., and Nelson, P., [*Active Control of Vibration*] (1996).

[11] Griffin, S., Gussy, J., Lane, S. A., Henderson, B. K., and Sciulli, D., "Virtual skyhook vibration isolation system," *Journal of Vibration and Acoustics* **124**(1), 63–67 (2002).

[12] Cazzulani, G., Resta, F., Ripamonti, F., and Zanzi, R., "Negative derivative feedback for vibration control of flexible structures," *Smart Materials and Structures* **21**, 1–10 (jun 2012).

[13] Yue, H., Lu, Y., Deng, Z., and Tzou, H., "Experiments on vibration control of a piezoelectric laminated paraboloidal shell," *Mechanical Systems and Signal Processing* **82**, 279–295 (2017).

[14] Baumann, O. N. and Elliott, S. J., "Destabilization of velocity feedback controllers with stroke limited inertial actuators," *The Journal of the Acoustical Society of America* **121**, EL211–EL217 (may 2007).

[15] Borgo, M. D., Tehrani, M. G., and Elliott, S., "Active nonlinear control of a stroke limited inertial actuator: Theory and experiment," *Journal of Sound and Vibration* **465**, 115009 (jan 2020).

[16] Lindner, D. K., Zvonar, G. A., and Borojevic, D., "Performance and control of proof-mass actuators accounting for stroke saturation," *Journal of Guidance, Control, and Dynamics* **17**, 1103–1108 (sep 1994).

[17] Cinquemani, S. and Resta, F., "A mechanical approach to the design of independent modal space control for vibration suppression," *Journal of Vibration and Acoustics* **135**, 1–12 (jun 2013).

[18] Benassi, L., Elliott, S. J., and Gardonio, P., "Active vibration isolation using an inertial actuator with local force feedback control," *Journal of Sound and Vibration* **276**, 157–179 (2004).

[19] Zimmerman, D. C. and Inman, D. J., "On the nature of the interaction between structures and proof-mass actuators," *Journal of Guidance* **13**, 82–87 (1989).

[20] Winberg, M., Johansson, S., and Claesson, I., "Inertial mass actuators, understanding and tuning," *The Internation Institute of Acoustics and Vibration (IIAV)* , 331–338 (2004).

[21] Paulitsch, C., Gardonio, P., Elliott, S. J., Sas, P., and Boonen, R., "Design of a lightweight, electrodynamic, inertial actuator with integrated velocity sensor for active vibration control of a thin lightly-damped panel," *Proceedings of the 2004 International Conference on Noise and Vibration Engineering* , 239–254 (2004).

[22] Cinquemani, S. and Braghin, F., "Decentralized active vibration control in cruise ship funnels," *Ocean Engineering* **140**, 361–368 (2017).

[23] Zilletti, M., Elliott, S. J., Gardonio, P., and Rustighi, E., "Experimental implementation of a self-tuning control system for decentralized velocity feedback," *Journal of Sound and Vibration* **331**(1), 1–14 (2011).